Hindawi
Advances in Materials Science and Engineering
Volume 2018, Article ID 4265617, 11 pages
https://doi.org/10.1155/2018/4265617

Research Article

Research on the Cross Section Forming Quality of Three-Dimensional Multipoint Stretch Forming Parts

Jiaqi Yu,[1,2] Yi Li,[1,2] Fei Teng,[3] Jicai Liang,[1,4] Xiangfeng Lin,[1,2] Ce Liang,[1,2] Guangyi Chen,[3] and Guangping Sun[2]

[1]*Key Laboratory of Automobile Materials, Ministry of Education, Jilin University, Changchun, Jilin 130025, China*
[2]*College of Materials Science and Engineering, Jilin University, Changchun, Jilin 130025, China*
[3]*School of Automotive Engineering, Dalian University of Technology, Dalian, Liaoning 116000, China*
[4]*Roll Forging Institute, Jilin University, Changchun, Jilin 130025, China*

Correspondence should be addressed to Yi Li; henrylee@jlu.edu.cn

Received 15 December 2017; Revised 28 February 2018; Accepted 29 April 2018; Published 24 June 2018

Academic Editor: Donato Sorgente

This paper introduced the basic principle and main influencing factors of the three-dimensional multipoint stretch forming process and investigated the optimized scheme of the cross section forming quality. The main factors affecting the stretch forming process were studied by the orthogonal test through the numerical simulation technique. In the case of a good target shape, the best combination of forming parameters was established by using the range method. The cross-sectional distortion of the formed profile is the smallest when the prestretching amount is 1% of the profile length, the poststretching amount is 0.8% of the profile length, the number of the die heads is 12, and the friction coefficient is 0.15. The optimal combination of forming parameters was verified by the multipoint bending test.

1. Introduction

Stretch forming is a method of bending parts under a combination of stretching and bending moments. The most challenging problem in the automobile industry now is to reduce the consumption of gasoline. Therefore, lightweight structure design is attracting much attention, and the aluminum alloy is widely used due to its strong stiffness and lightweight [1]. Three-dimensional multipoint stretch forming is a rapid flexible forming technique which is different from the traditional bending forming. Its flexible bending head makes the bending radius change, so it can be widely applied to many profiles [2, 3]. In addition to the common problems such as wrinkle, springback, and fracture in sheet forming, there are some special problems in the forming parts, such as cross-sectional distortion. The common problem of thin-walled section stretch forming is the cross-sectional distortion, and the main defects are collapse and bulging [4–8].

In order to achieve the skeleton of the spatial structure with complex three-dimensional surface, many scholars had done some researches. By using the numerical simulation technology, Paulsen and Welo made an arrangement for the degree of factors affecting the distortion on the cross section [9]. Miller et al. did a detailed research on the influence of stretch-bending process parameters on formability, then optimized the parameters, and got the conclusion that the tension force can reduce springback [10]. Paulsen and Welo discussed the collapse of the cross section and obtained a fairly complex equation set [11]. Chunguo et al. systematically studied the basic theory and technology of sheet metal multipoint forming process and named the adjustable forming method "multipoint forming" for the first time [12]. A finite element simulation trajectory design method based on deformation control was proposed by Li et al. [13]. For different loading methods of two different aluminum profiles, Clausen et al. used the experimental method and the finite element

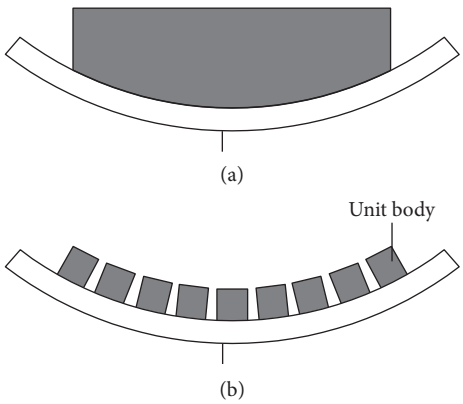

Figure 1: Comparison of traditional die and multipoint die. (a) Conventional die forming. (b) Flexible die forming.

analysis, and they found that the cross-sectional geometry and prestretching affect the distortion greatly [14]. Diao et al. came up with the mechanical property parameters of materials through the relevant mechanical experiments of rectangular aluminum alloy profiles [15].

In this paper, under the precondition that the target shape was well bent, the numerical simulation technology was used to simulate the stretch forming process according to the characteristics that the section of rectangular thin-walled hollow aluminum alloy is easy to deform. During the stretch forming process, the main process parameters influencing the cross-sectional distortion were studied by the orthogonal test; then, the effect of a single factor was discussed; and finally, the optimal combination of process parameters by the range method was determined.

2. Three-Dimensional Multipoint Stretch Forming Process

2.1. Basic Principle. Multipoint forming (MPD) is an advanced forming technique which is based on the principle of flexible multipoints forming technology. The traditional monolithic die is discretized to form a flexible die with a variable shape and adjustable height. It can be adjusted in horizontal and vertical directions to achieve three-dimensional stretch bending [16]. Compared with the traditional die, the unit body of three-dimensional stretched die has the advantages of wide processing profile length, simple shape adjustment, and application of various types of cross sections. The reconfigurable die with multiple units are used to reconstruct the die surface by changing the space position during the flexible stretch forming process, as shown in Figure 1 [17, 18].

The flexible stretch forming machine is made of the proper installation of several die heads on the worktable of the bending machine combining with the traditional stretch forming method, and the structure is shown in Figure 2.

2.2. Main Factors Affecting the Multipoint Stretch Forming. The profile stretching is usually stretched to the plastic state and is fitted on the contact surface of the bending die to get

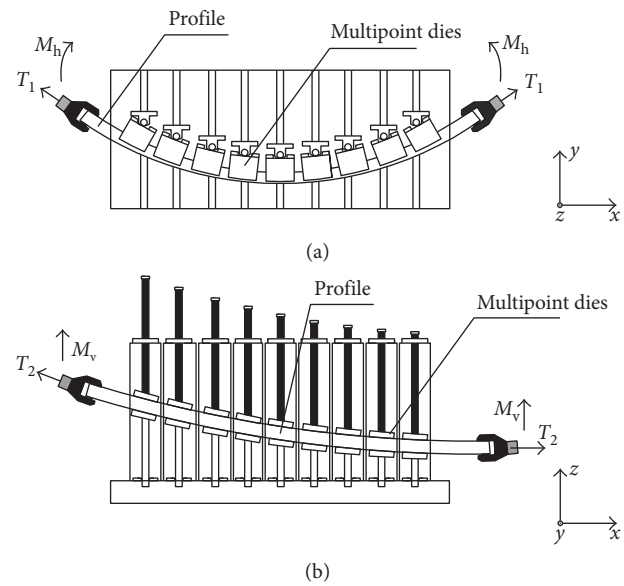

Figure 2: Structure drawing of three-dimensional stretch forming equipment: bending forming in (a) horizontal and (b) vertical stages.

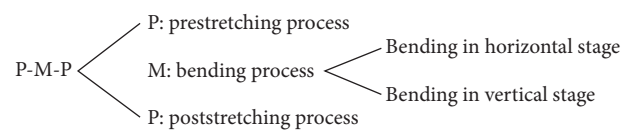

Figure 3: P-M-P process flow diagram.

the final shape. The most important cross-sectional distortions during bending are collapse and bulging, so it is necessary to find a practical solution.

The main forming process of three-dimensional stretch forming is divided into three steps: prestretching process, bending process, and poststretching process, that is, the P-M-P method. First, the clamps are controlled along the displacement direction of the profile for the poststretching process. The amount of prestretching should make the plastic deformation of the profile appropriate because too much prestretching will lead to section collapse and fracture of the profile. Second, the clamps drive the profile to fit the dies. The bending process includes two stages: bending in horizontal and bending in vertical. The profile is bent in the horizontal plane first and is bent along the z-axis then. Last, the poststretching is done for the curved profile to improve the forming precision. The reference point of the clamp controls the profile to move in the direction of the part. In the whole process of bending, the size of the friction coefficient and the number of multipoint die heads also affect the quality of forming parts. The P-M-P process flow diagram is shown in Figure 3.

3. Numerical Simulation

The finite element analysis method can simplify the profile reasonably. The finite element model can be used to study

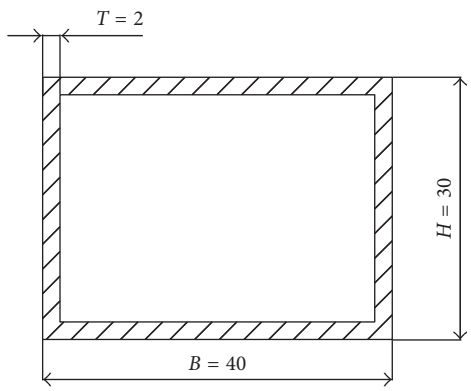

Figure 4: Sectional geometry.

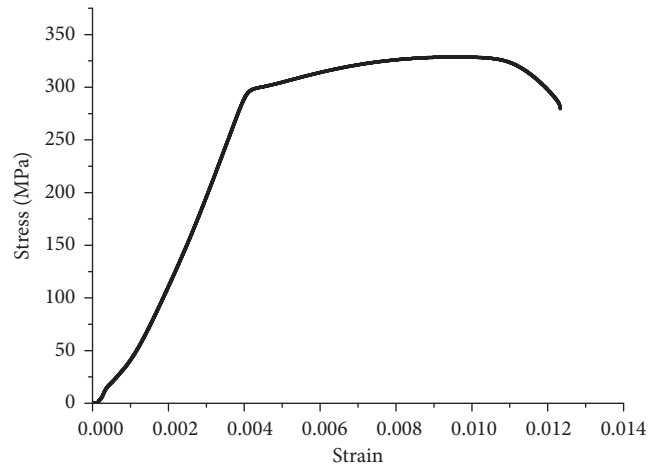

Figure 5: Stress-strain curve.

the stress and strain distribution, springback, wrinkling, rupture, collapse, bulging, and other problems during the forming process. By changing the process parameters, the influence of the parameters on the forming quality was studied, so that the adjustment can be made properly to get the optimal solution into actual experimental production. In this paper, the three-dimensional multipoint stretch forming process of the aluminum alloy rectangular profile was numerically simulated by using the finite element analysis software ABAQUS. The section size is shown in Figure 4 (unit: mm). This paper used the aluminum alloy AA6082 as the experiment profile, its stress-strain curve is shown in Figure 5, and the material parameter is shown in Table 1. The length of the profile is 3200 mm. The target bending radius is 2500 mm, and both the horizontal bending angle and the vertical bending angle are 30°. The experiment is mainly to form the whole profile by stretch forming.

3.1. Reasonable Simplification of Flexible Three-Dimensional Stretch Forming. The flexible three-dimensional stretch forming process of the profile is a complex nonlinear springback forming problem, which includes the nonlinearity of materials and the nonlinearity of boundary conditions and so on. A too complicated model not only prolongs the calculation time but also leads to the inaccuracy of the calculation results. In order to get accurate simulation, the finite element model of flexible three-dimensional stretch forming was reasonably simplified.

3.1.1. Simplification of Stretch Forming Process. In the finite element analysis of flexible stretch forming, it is important to simulate the profile gradually fitting the flexible dies under the action of the linear displacement of the clamps. The unnecessary components of the bending machine were simplified; that is, to say, the forming process of stretch bending can only be driven by the clamp to fit the die body.

3.1.2. Simplification of Operation Process. Half of the profile was selected for simulation in consideration of the symmetry of the profile and operation, and it was also convenient to observe the distortion of the cross section and save time. Because of the symmetry of the profile and the operation, in the finite element analysis of the three-dimensional multipoint flexible stretch forming, half of the dies, clamps, and profile which were selected to simulate can facilitate the observation of cross-sectional distortion and shorten the calculation time. Therefore, the finite element model presented in this paper is composed of one-half of each component.

Table 1: Material parameter.

E (MPa)	ν	σ_0 (MPa)	σ_b (MPa)	ρ (kg·m^{-3})
71000	0.345	295	328	2710

Note: E represents the modulus of elasticity, ν represents the Poisson ratio, σ_0 represents the yield stress, σ_b represents the tensile strength, and ρ represents the density.

3.1.3. Simplification of Shape. Since the profile has the regular rectangular section, in the finite element model, the shape and the size of the aluminum profile were designed in 1 : 1 scale according to the actual size, and the three-dimensional solid element was selected. The shape of the die that controls the horizontal bending on the bending machine is shown in Figure 7. The limit screw that controls vertical bending on the bending machine was defined in the same shape as the die unit in the model and was simplified as a discrete rigid body. The clamps used the same shape of rectangular three-dimensional shell structure as the profile, with a length of 50 mm. Figure 6 is the assembly sketch of the profile, and Figure 7 is the parts diagram. The target shape of the aluminum profile is shown in Figure 8.

3.1.4. Reasonable Mesh Partitioning. Because the profiles, clamps, and multipoint die heads in this paper are all regular shapes, this paper adopted structured grid technology. The aluminum profile unit used a hexahedron structure, and the wall thickness was divided into a layer of mesh; that is, the mesh size was 2×2 mm, and the mesh size in length and width direction was 2.5×2.5 mm. Since the horizontal multipoint die, vertical multipoint die, and clamp have

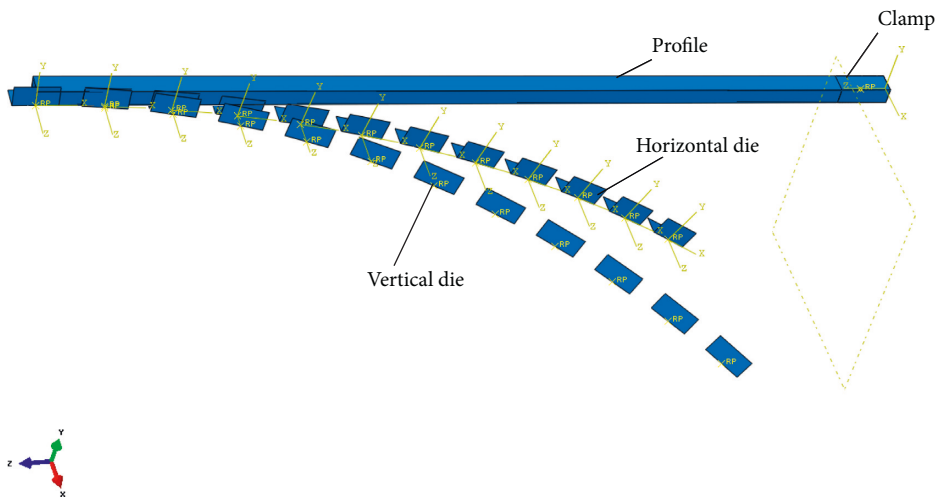

Figure 6: Assembly sketch of the profile.

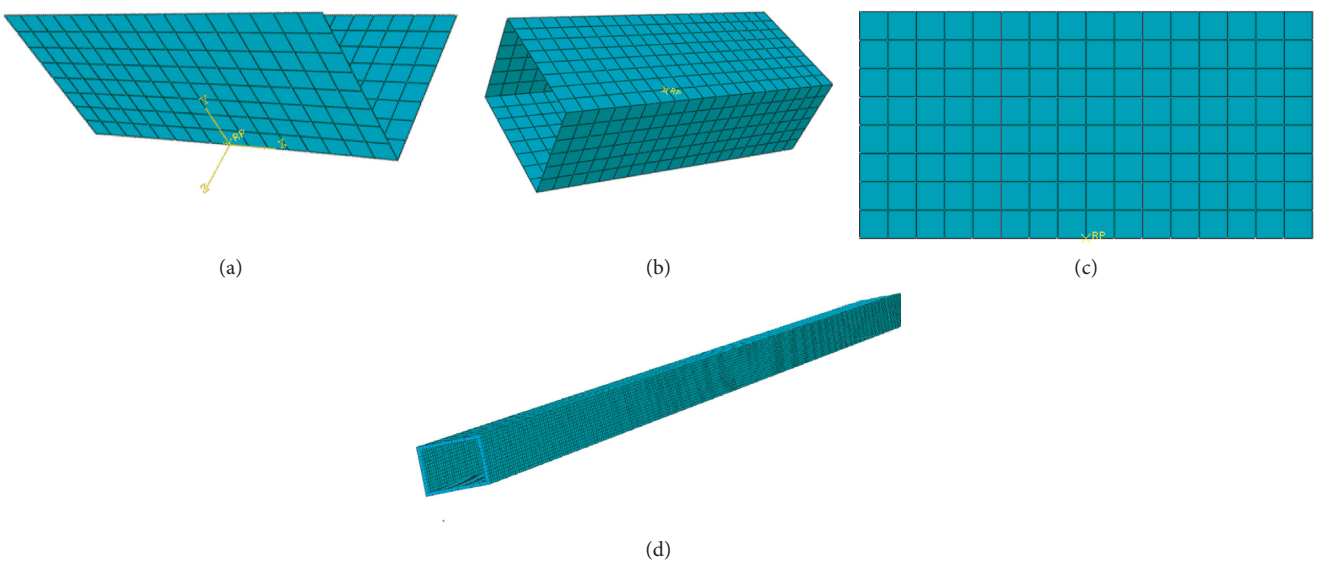

Figure 7: Parts diagram: (a) horizontal die; (b) clamp; (c) horizontal die; (d) profile.

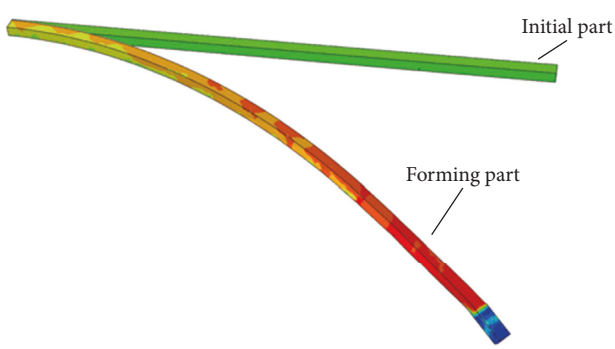

Figure 8: The target shape of the aluminum profile.

a relatively small influence on the calculation results and are not the main part of the study, the mesh size was designed to be 5×5 mm to save calculation time, such as Figure 7.

The finite element model was divided into three submodels and five analytic steps, which were defined as the horizontal bending model, vertical bending model, and poststretching model, respectively. The horizontal bending model included the initial analysis step, the prestretching process, and the horizontal bending stage. The vertical bending model included the vertical bending stage. And the poststretching model included the poststretching process. After completing each model task successfully, it was used as a predefined field to start the next model run.

3.2. The Orthogonal Test. The orthogonal test is a design method which is based on the orthogonality of the data to design the scheme. It has the advantage of being able to obtain reliable and representative test results in test times as few as possible. Through the analysis and integration of the test results, the best test conditions are selected as the optimal level combination of each factor. The orthogonal test

Table 2: Orthogonal test.

Level	Factor			
	A	B	C	D
1	0.8% L	0.8% L	6	0.05
2	1.0% L	1.0% L	8	0.1
3	1.2% L	1.2% L	10	0.15
4	1.4% L	1.4% L	12	0.2

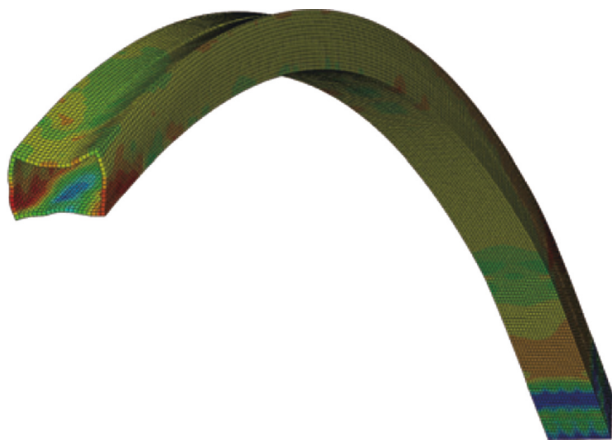

Figure 9: Numerical simulation of the profile deformation.

is beneficial to improve production efficiency, shorten working time, and improve process quality, so it is widely used in the field of automobile manufacture and aerospace to deal with multifactor problems.

Proper prestretching and poststretching will affect the distortion of the cross section and then change the precision of the forming part. The number of die heads also affects the wrinkling and deformation of the profile during the bending process. Therefore, this paper focused on the experimental factors including prestretching, poststretching, the number of die heads, and the friction coefficient, defining A as the amount of prestretching, B as the amount of poststretching, C as the number of die heads, and D as the amount of friction coefficient. The assessment index was the cross-sectional distortion of the stretch forming parts, and the collapse rate and the bulging rate were taken as the evaluation criteria. Four experimental factors were selected. Therefore, the orthogonal test was designed with four factors and four levels. Altogether, 16 groups of experiments were carried out, which is shown in Table 2.

3.3. Assessment Index. The method of quantitative analysis was used to deal with the distortion of the cross section. Select the maximum level of various factors as a parametric combination for the boundary simulation. The combination was $C = 12$, $A = B = 1.4\%$ L, and $D = 0.2$. Figure 9 is the numerical simulation of the profile deformation. To facilitate observation, the distortion diagram of the cross section is plotted as shown in Figure 10. What this paper mainly measured was how the section changes after the horizontal bending, the vertical bending, and the poststretching.

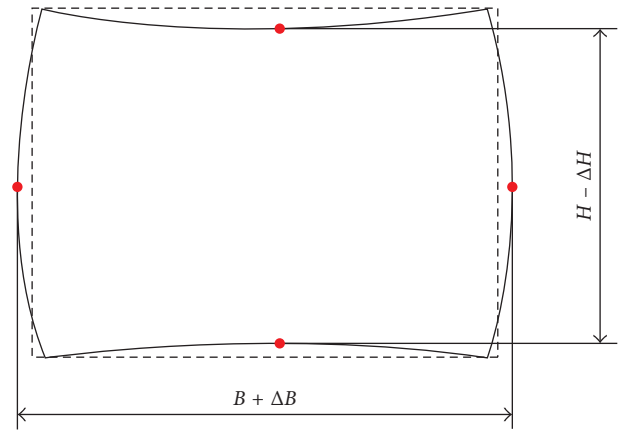

Figure 10: Distortion map of the cross section.

Table 3: Range table.

Index		A	B	C	D
δ_h	$k1$	0.0845	0.0843	0.0962	0.0846
	$k2$	0.0817	0.0875	0.0857	0.0869
	$k3$	0.0904	0.0884	0.0823	0.0835
	$k4$	0.0885	0.0849	0.0810	0.0902
	R	0.0087	0.0040	0.0152	0.0067
δ_v	$k1$	0.1188	0.1125	0.1357	0.1113
	$k2$	0.1096	0.1152	0.1106	0.1204
	$k3$	0.1204	0.1182	0.1109	0.1080
	$k4$	0.1168	0.1198	0.1084	0.1259
	R	0.0108	0.0073	0.0273	0.0179
δ_p	$k1$	0.1212	0.1166	0.1392	0.1274
	$k2$	0.1162	0.1224	0.1224	0.1280
	$k3$	0.1293	0.1257	0.1166	0.1117
	$k4$	0.1170	0.1188	0.1054	0.1165
	R	0.0131	0.0091	0.0338	0.0163
η_h	$k1$	0.0177	0.0163	0.0184	0.0185
	$k2$	0.0155	0.0162	0.0171	0.0165
	$k3$	0.0154	0.0163	0.0160	0.0149
	$k4$	0.0166	0.0164	0.0136	0.0151
	R	0.0023	0.0002	0.0048	0.0036
η_v	$k1$	0.0124	0.0127	0.0119	0.0111
	$k2$	0.0120	0.0102	0.0113	0.0112
	$k3$	0.0096	0.0108	0.0120	0.0109
	$k4$	0.0120	0.0124	0.0109	0.0134
	R	0.0028	0.0024	0.0011	0.0025
η_p	$k1$	0.0263	0.0240	0.0236	0.0247
	$k2$	0.0224	0.0219	0.0236	0.0253
	$k3$	0.0221	0.0249	0.0259	0.0219
	$k4$	0.0253	0.0253	0.0230	0.0242
	R	0.0041	0.0034	0.0030	0.0033

Note: δ_h represents the collapse rate in the horizontal stage, δ_v represents the collapse rate in the vertical stage, δ_p represents the collapse rate in the poststretching process, η_h represents the bulging rate in the horizontal stage, η_v represents the bulging rate in the vertical stage, and η_p represents the bulging rate in the poststretching process.

Measure the outermost midpoint change in the symmetry section. The gap amount (ΔB and ΔH) was used to describe the amount of profile cross-sectional distortion. Among them, the collapse rate $\delta = \Delta H/H$, and the bulging rate $\eta = \Delta B/B$.

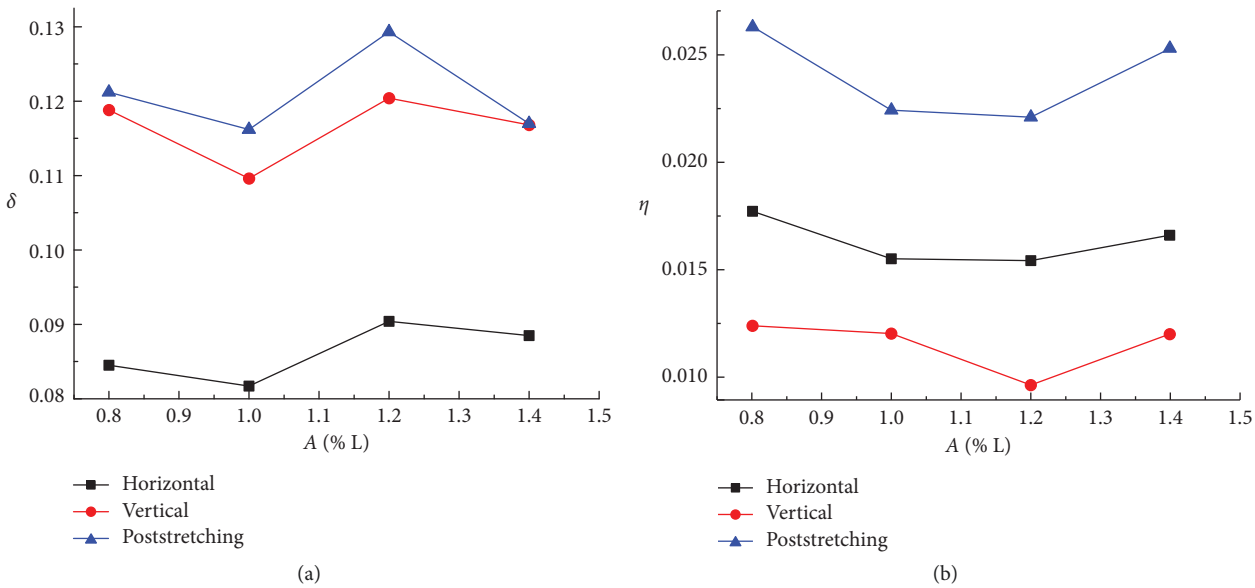

Figure 11: Influence of prestretching on cross-sectional distortion during each process.

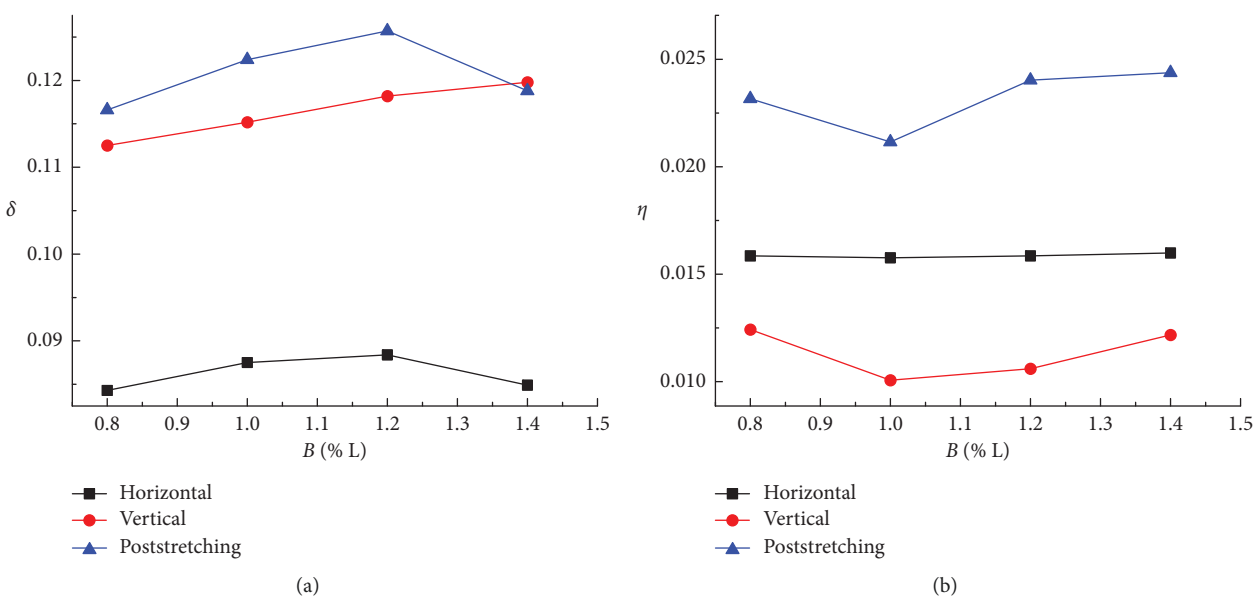

Figure 12: Influence of poststretching on cross-sectional distortion during each process.

4. Results and Analysis

4.1. Orthogonal Test Result. The orthogonal test method not only makes the plan have some advantages but also reduces the test points, so that a small number of experiments can get rich information, control the test interference effectively, and get a comprehensive conclusion [19]. The range method is an analysis method which is easy to grasp and has less calculation. It is used to screen the initial test, to seek the optimal production condition and the process and so on. The cross-sectional distortion of the horizontal bending process, the vertical bending process, and the poststretching process was measured. And the average number of arithmetical number corresponding to the level number was recorded as ki ($i = 1, 2, 3, 4$). The difference between the max $\{ki\}$ and the min $\{ki\}$ on any column was the extreme R. Data record analyses in Table 3 are obtained by the range method.

4.2. Influence of Single Factor on Cross-Sectional Distortion of Each Process. The following graphs are the corresponding trend maps at different levels of influence factors. This paper discussed the cross-sectional variation trend in bending in the horizontal, vertical, and poststretching process (defining bending in the horizontal stage, bending in the vertical stage,

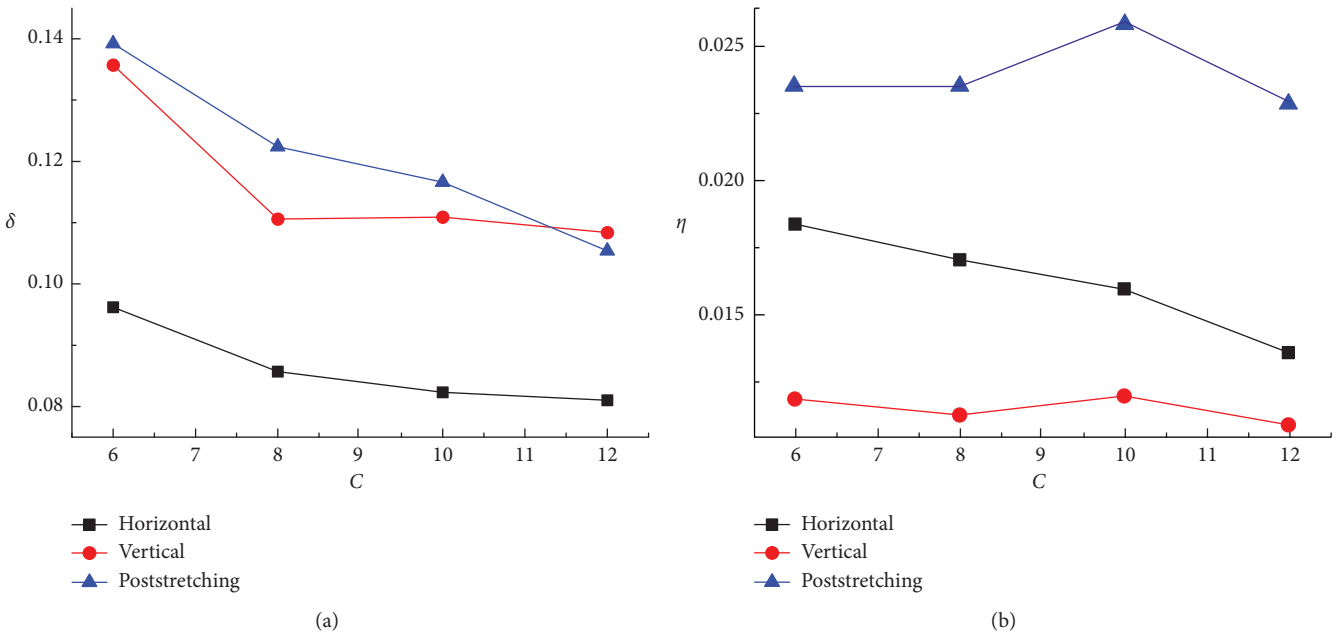

Figure 13: Influence of the number of die on cross-sectional distortion during each process.

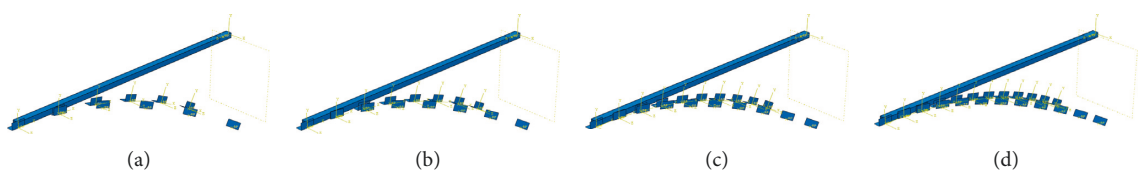

Figure 14: Assembly drawing with different number of die heads: (a) $C = 6$; (b) $C = 8$; (c) $C = 10$; (d) $C = 12$.

and poststretching process as two processes or three stages). The horizontal coordinate is the level, and the longitudinal coordinate is a cross section variable obtained by the use of the range method.

4.2.1. Influence of Prestretching. Figure 11 is a trend diagram of the variation of the cross-sectional distortion with the amount of prestretching during the stretch forming. As can be seen from Figure 11, during the bending process, when the prestretching $A = 1.0\%$ L (Figure 11(a)), δ is the smallest, and the tendency of bending in the horizontal stage, bending in the vertical stage, and the poststretching process is almost the same. They both reduce, then increase, and finally decrease. When the prestretching $A = 1.2\%$ L (Figure 11(a)), δ is the biggest. η is the smallest when $A = 1.2\%$ L (Figure 11(b)). At the same time, the effect of prestretching on the rate of bulging does not have a large amount on collapse.

4.2.2. Influence of Poststretching. The changing trend of cross-sectional distortion with the amount of poststretching during the stretch forming process is shown in Figure 12. As can be seen from Figure 12(a), δ increases when B increases from 0.8% L to 1.2% L during the both three stages. When B increases to 1.4% L, δ decreases in the vertical bending stage and poststretching process. δ becomes larger in the horizontal bending stage. The reason is that the amount of poststretching was applied to the poststretching process and that it had a great influence on the distortion. δ is the smallest when $B = 0.8\%$ L during the two processes. It can be seen from Figure 12(b) that the influence of the poststretching on the bulging rate is not obvious in the horizontal direction. The others have obvious fluctuations. In the vertical bending stage, bulging η reduces and then increases gradually. As for the poststretching process, it is a bit different from the bending in the vertical stage, and when $B > 1.2\%$ L, η decreases slightly. But η is the smallest when $B = 1.0\%$ L during the two processes.

4.2.3. Influence of the Number of Die Heads. The changing trend of cross-sectional distortion with the number of die heads during the stretch forming process is shown in Figure 13. As can be seen from Figure 13(a), the collapse rate δ decreases with the increase of C in both horizontal and vertical stages, which can reflect the advantage of multipoint flexible forming. And the number of die heads can reduce the collapse effectively. As shown in Figure 13(b), the vertical bending and the poststretching process tend to have similar effects on the bulging rate η, but the horizontal bending is

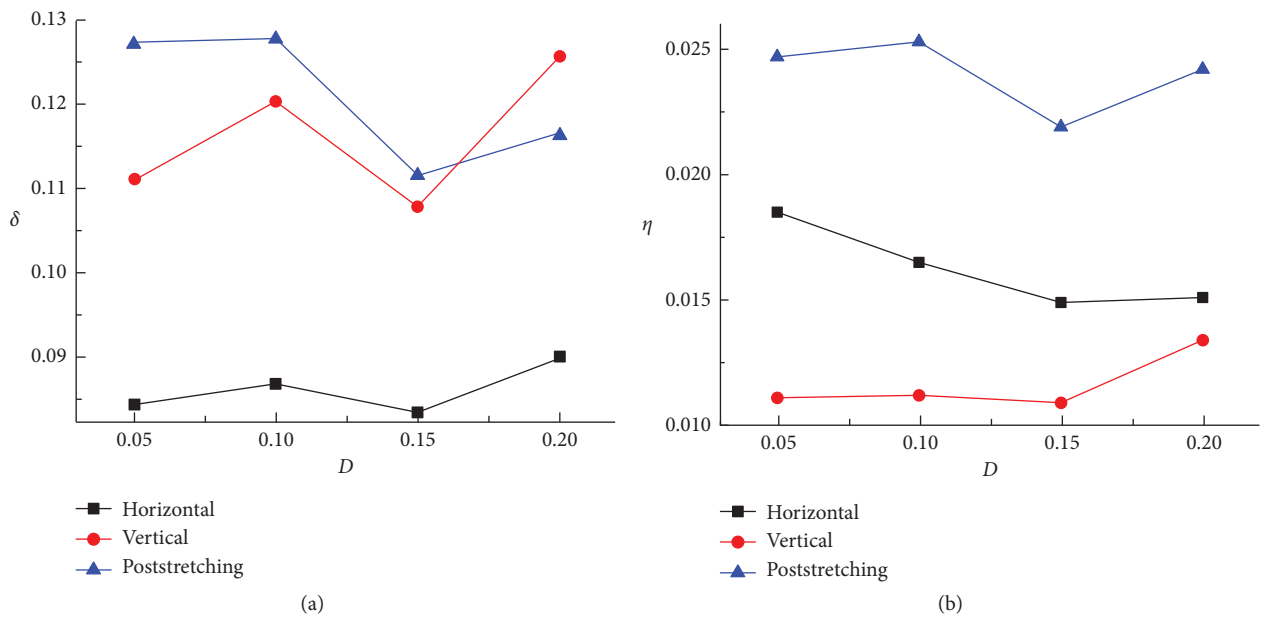

Figure 15: Influence of friction coefficient on cross-sectional distortion during each process.

different from them. In general, the distortion of the cross section is the largest when $C = 6$ and the distortion of the cross section is the smallest when $C = 12$. Figure 14 is the assembly drawing with different number of die heads.

4.2.4. The Influence of Friction Coefficient. Figure 15 is the influencing trend of the friction coefficient on the cross-sectional distortion during the stretch forming process. From Figure 15(a), when $D = 0.15$, δ is the smallest in the both two process. During the bending process, the cross-sectional distortion has a upward trend, then decreases, and finally increases. From Figure 15(b), as for the effect of friction coefficient on the horizontal stage, when the friction between 0.12 and 0.15 increases, the bulging rate becomes smaller. The tendency of bending in the vertical stage and the poststretching process are almost the same. They both increased, then reduced, and finally decreased. Generally speaking, when $D = 0.15$, the overall distortion of the cross section is minimal.

4.3. Process Parameters Optimization and Verification Experiment. The analysis from 4.2 is based on the size of the collapse rate and the bulging rate; therefore, the smaller the amount, and the better the result. The best combination of process parameters is $C4D3$, where $C = 12$ and $D = 0.15$. Further analyses are needed for the selection of prestretching and poststretching. Comparing ki of the factors A and B in Table 3 (the smaller ki indicates the smaller degree of influence on behalf of this level) and the combination of the prestretching and poststretching are designed in Table 4.

From Table 4, it can be seen that the best combination of the bending process for reducing the collapse rate is $A2B1$, and the best combination of the stretch forming process for reducing bulging is $A3B2$. The comparison of several groups of data shows that not all the indicators are consistent, but the general trend is the same. In order to find the optimal combination, the following two sets of process parameters are numerically simulated to determine the optimal combination, and the experimental verification is carried out in the stretch forming test.

Table 4: Optimal parameter combination of factors A and B in each process.

Index	A	B	Combination
δ_h	$k2 < k1 < k4 < k3$	$k1 < k4 < k2 < k3$	$A2B1$
δ_v	$k2 < k4 < k1 < k3$	$k1 < k2 < k3 < k4$	$A2B1$
δ_p	$k2 < k4 < k1 < k3$	$k1 < k4 < k2 < k3$	$A2B1$
η_h	$k3 < k2 < k4 < k1$	$k2 < k1 < k3 < k4$	$A3B2$
η_v	$k3 < k2 = k4 < k1$	$k2 < k3 < k4 < k1$	$A3B2$
η_p	$k3 < k2 < k4 < k1$	$k2 < k1 < k3 < k4$	$A3B2$

Figure 16: Three-dimensional multipoint stretch forming test.

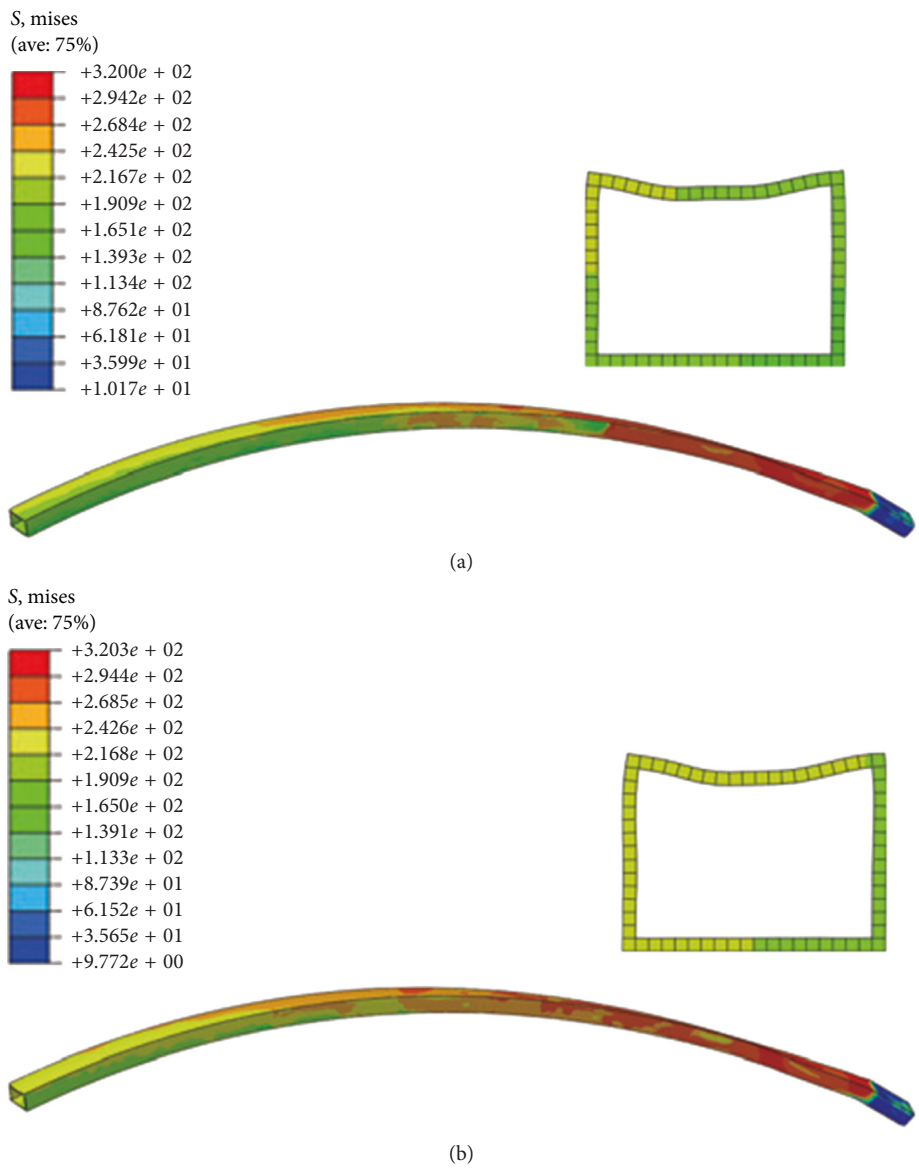

Figure 17: Numerical simulation of the two combinations: (a) *A*2*B*1*C*4*D*3. (b) *A*3*B*2*C*4*D*3.

According to the combination of the two sets of parameters obtained from the simulation, the forming test is arranged to verify the simulation results and the optimal combination of parameters is discussed (the profile-related parameters used in the stretch-bending forming test are consistent with the simulation parameters). Figure 16 is a multipoint stretch forming test. Figure 18 shows the cross-sectional distortion of the two process parameters.

As can be seen from the stress clouds of the simulation in Figure 17, on the one hand, the stress distribution at section *A*2*B*1*C*4*D*3 is mainly green, while that at section *A*3*B*2*C*4*D*3 is yellow as a whole. From the distribution of stress cloud, the yellow part of the stress value is greater than the green part of the stress value; therefore, the overall stress distribution of *A*2*B*1*C*4*D*3 is smaller than that of *A*3*B*2*C*4*D*3. On the other hand, the cross-sectional distortion of *A*2*B*1*C*4*D*3 is smaller than *A*3*B*2*C*4*D*3. So the optimal combination of the finite element simulation results is *A*2*B*1*C*4*D*3. As shown in Figure 18, the cross-sectional distortion of *A*2*B*1*C*4*D*3 is smaller than that of *A*3*B*2*C*4*D*3 in each process step of the forming test, so the best combination is *A*2*B*1*C*4*D*3 which is in agreement with the results obtained from the numerical simulation.

5. Conclusion

This paper studied the three-dimensional multipoint stretch forming of the aluminum alloy rectangular profile and used the finite element analysis method to investigate the influence of prestretching, poststretching, the number of die heads, and the coefficient of friction on the distortion of the

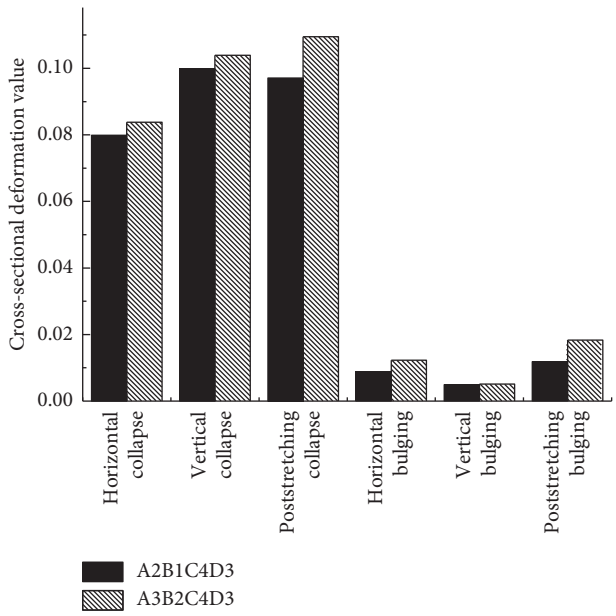

Figure 18: Cross-sectional distortion of two process parameters of forming parts.

cross section. The optimal combination of process parameters was determined and was verified by the forming test.

(1) The effect of collapse on the profile is greater than bulging. The collapse rate decreases with the increase of the prestreching amount from 0.8% L to 1.0% L. As the prestretching amount continues to increase, the cross-sectional distortion becomes larger and then decreases slightly. When prestretching amount is 1.2% L, the collapse rate is the smallest.

(2) After unloading, the profile enters the stage of the poststretching process. When the amount of the poststretching amount is increased from 0.8% L to 1.2% L, the collapse rate increases generally. Therefore, the larger the poststretching amount, the larger the collapse rate. However, there are little fluctuations during the horizontal bending process on the bulging problem.

(3) The number of die heads has great influence on the accuracy of profile forming. When the number of die heads increase from 6 to 12, the collapse obviously decreases and the cross-sectional distortion is obviously improved.

(4) When the friction coefficient increases from 0.01 to 0.2, the cross-sectional distortion in the horizontal direction is not large, but when it reaches 0.15, the overall cross-sectional distortion becomes small.

(5) By taking the orthogonal test and forming test on rectangular hollow section profile, the optimal combination of three-dimensional multipoint stretch forming is as follows: the prestretching amount is 1.0% L, the poststretching amount is 0.8% L, the number of die heads is 12, and the friction coefficient is 0.15.

Conflicts of Interest

The authors declare that they have no conflicts of interest.

References

[1] M. Geiger and A. Sprenger, "Controlled bending of aluminum extrusions," *CIRP Annals*, vol. 47, no. 1, pp. 197–202, 1998.

[2] L. Jicai, T. Fei, G. Song et al., "Key technologies research on the iterative die-face adjustment in the forming process of flexible three-dimensional stretch-bending," *Journal of Mechanical Engineering*, vol. 49, no. 17, pp. 187–192, 2013.

[3] G. Song, L. Jicai, C. Guangyi et al., "Rapid adjusting of fundamental units in process of flexible 3D stretch-bending," *Journal of Jilin University: Engineering and Technology Edition*, vol. 44, no. 6, pp. 1723–1728, 2014.

[4] L. Zhiwei, L. Mingzhe, and H. Qigang, "Multi-point forming with wrinkle resistance function and its forming accuracy," *Journal of Mechanical Engineering*, vol. 48, no. 12, pp. 56–62, 2012.

[5] G. Zhengwei, C. Zhongyi, and X. Hong, "Numerical analysis and optimization of stretch-bending process," *Journal of Jilin University: Engineering and Technology Edition*, vol. 39, no. 5, pp. 1167–1171, 2009.

[6] Z.-Y. Cai, S.-H. Wang, X.-D. Xu, and M.-Z. Li, "Numerical simulation for the multi-point stretch forming process of sheet metal," *Journal of Materials Processing Technology*, vol. 209, no. 1, pp. 396–407, 2009.

[7] L. G. Brazier, "On the flexure of thin cylindrical shells and other "thin" sections," *Proceedings of the Royal Society of London*, vol. 116, no. 773, pp. 104–114, 1927.

[8] X.-L. Zhang, X.-X. Li, X.-B. Zhou, and M. Jin, "Finite element simulation for stretch-wrap bending of aluminum profile with complex cross section," *Journal of Plasticity Engineering*, vol. 11, no. 4, pp. 44–47, 2004.

[9] F. Paulsen and T. Welo, "Application of numerical simulation in the bending of aluminum-alloy profiles," *Journal of Materials Processing Technology*, vol. 58, no. 2-3, pp. 274–285, 1996.

[10] J. E. Miller, S. Kyriakides, and A. H. Bastard, "On bend-stretch forming of aluminum extruded tubes I experiments," *International Journal of Mechanical Sciences*, vol. 43, no. 5, pp. 1283–1317, 2001.

[11] F. Paulsen and T. Welo, "Cross-sectional deformations of rectangular hollow sections in bending: part II analytical models," *International Journal of Mechanical Sciences*, vol. 43, no. 1, pp. 131–152, 2001.

[12] L. Chunguo, L. Mingzhe, C. Zhongyi, and C. Qingmin, "Research on multi-point closed-loop forming of 3D sheet metal parts," *China Mechanical Engineering*, vol. 11, no. 12, pp. 1326–1329, 2000.

[13] X. Li, X. Zhou, C. Jin, and C. Hao, "Design of stretch bending trajectory based on finite element simulation for three-dimensional profile parts," *Acta Aeronautica et Astronautica Sinica*, vol. 30, no. 3, pp. 544–550, 2009.

[14] A. H. Clausen, O. S. Hopperstad, and M. Langseth, "Stretch bending of aluminum extrusions for car bumpers," *Journal of Materials Processing Technology*, vol. 102, no. 1, pp. 241–248, 2000.

[15] K. Diao, X. Zhou, X. Li, and B. Criqui, "An investigation of material properties of aluminum extrusion 6082(T5) and the establishment of FLD," *China Mechanical Engineering*, vol. 15, no. 13, pp. 1202–1204, 2004.

[16] L. Yi, L. Jicai, T. Fei, L. Ce, and Y. Jiaqi, "Multi-phase iterative compensation method of die shape optimization for multi-point stretch bending profile," *Journal of Jilin University: Engineering and Technology Edition*, vol. 46, no. 6, pp. 1961–1966, 2016.

[17] J.-C. Liang, S. Gao, F. Teng, and X.-J. Song, "Flexible 3D stretch-bending technology for aluminum profile," *International Journal of Advanced Manufacturing Technology*, vol. 71, no. 9–12, pp. 1939–1947, 2014.

[18] X. P. Gong, M. Z. Li, Z. Q. Hu, and Z. Y. Cai, "Research on continuous multi-point forming technology for three-dimensional sheet metal," *International Journal of Materials and Product Technology*, vol. 38, no. 2-3, pp. 210–222, 2010.

[19] L. Jicai, S. Mei, L. Yi et al., "Influence factor analysis of gas fingering defect in gas-assisted injection dieing of automobile handle," *Journal of Mechanical Engineering*, vol. 44, no. 12, pp. 303–313, 2008.